

Solid-State NMR

How to cite:

International Edition: doi.org/10.1002/anie.202114103

German Edition: doi.org/10.1002/ange.202114103

Highly Efficient Polarizing Agents for MAS-DNP of Proton-Dense Molecular Solids

Rania Harrabi, Thomas Halbritter, Fabien Aussenac, Ons Dakhlaoui, Johan van Tol, Krishna K. Damodaran, Daniel Lee, Subhradip Paul, Sabine Hediger, Frederic Mentink-Vigier,* Snorri Th. Sigurdsson,* and Gaël De Paëpe*

Abstract: Efficiently hyperpolarizing proton-dense molecular solids through dynamic nuclear polarization (DNP) solid-state NMR is still an unmet challenge. Polarizing agents (PAs) developed so far do not perform well on proton-rich systems, such as organic microcrystals and biomolecular assemblies. Herein we introduce a new PA, cAsymPol-POK, and report outstanding hyperpolarization efficiency on 12.76 kDa U-¹³C,¹⁵N-labeled LecA protein and pharmaceutical drugs at high magnetic fields (up to 18.8 T) and fast magic angle spinning (MAS) frequencies (up to 40 kHz). The performance of cAsymPol-POK is rationalized by MAS-DNP simulations combined with electron paramagnetic resonance (EPR), density functional theory (DFT) and molecular dynamics (MD). This work shows that this new biradical is compatible with challenging biomolecular applications and unlocks the rapid acquisition of ¹³C–¹³C and ¹⁵N–¹³C correlations of pharmaceutical drugs at natural isotopic abundance, which are key experiments for structure determination.

Introduction

Solid-state nuclear magnetic resonance (ssNMR) with magic angle spinning (MAS) is a powerful and versatile spectroscopy for studying structure and dynamics at the atomic level.^[1,2] Despite its strengths, ssNMR often suffers from a lack of sensitivity when detecting nuclei with low gyromag-

netic ratio, low isotopic abundance, or carrying a nuclear quadrupole moment. These limitations can be overcome through the use of hyperpolarization techniques, such as high-field dynamic nuclear polarization under MAS (MAS-DNP),^[3–5] which has emerged as a powerful approach to perform previously impossible NMR experiments for a wide range of applications from materials to life science.^[6–9] The MAS-DNP amplification effect is based on the use of special paramagnetic centers, called polarizing agents (PAs), which act as a polarization source under high frequency microwave irradiation to hyperpolarize nuclear spins.^[5,10,11]

These developments at high magnetic field, pioneered by the Griffin group at MIT, have required the development of dedicated instrumentation such as continuous wave high-power high-frequency gyrotron microwave sources, low temperature MAS-DNP probes, as well as efficient PAs.^[5,10,12] This last research axis witnessed an important milestone in the early 2000s with the introduction of chemically-bound bis-nitroxides^[13] that can provide a substantial improvement in Cross Effect (CE) MAS-DNP efficiency. Since then, considerable efforts have been devoted to further improvements. Today, the most used biradicals for CE MAS-DNP are AMUPol^[14] in aqueous solutions and TEKPol^[15] in organic solvents, owing to their good efficiency and commercial availability. Although these radicals provide relatively high enhancement factors ($\epsilon_{\text{On/Off}}$) at 9.4 T and 100 K,^[14] they exhibit a marked depolarization effect (ϵ_{depo}),^[16] and a relatively long nuclear spin hyperpolarization build-up time (T_{B}), and thus overall, a limited sensitivity gain. In addition, the CE MAS-DNP efficiency^[17,18] of these biradicals tends to decrease significantly with increasing magnetic field (> 9.4 T) and MAS frequency (> 10 kHz).^[19]

To alleviate these limitations, hetero-biradicals were recently introduced, in which a carbon-based radical is linked to a nitroxide.^[19] The first example of an efficient hetero-biradical for water-based applications was TEMTriPol-I,^[19] shown to perform well at high magnetic field^[19,20] while having a limited depolarization effect and requiring less microwave power.^[20] The hetero-structure was recently extended to the NaTriPol family by functionalizing the TEMTriPol-I linker, which limits the propensity of the radical to aggregate.^[21] Furthermore, BDPA-nitroxide mixed biradicals, known as the HyTEK family, were also introduced for organic solvent-based applications.^[22,23] Advanced numerical simulations can help guide the design of new PAs,^[24] as illustrated recently with a family of bis-nitroxides,

[*] R. Harrabi, O. Dakhlaoui, Dr. D. Lee, Dr. S. Paul, Dr. S. Hediger,

Dr. G. De Paëpe
 Univ. Grenoble Alpes, CEA, CNRS, IRIG, MEM
 38000 Grenoble (France)
 E-mail: gael.depaepe@cea.fr

Dr. T. Halbritter, Prof. K. K. Damodaran, Prof. S. T. Sigurdsson
 University of Iceland, Department of chemistry, Science Institute,
 Dunhaga 3, 107 Reykjavik (Iceland)
 E-mail: snorrisi@hi.is

Dr. F. Aussenac
 Bruker Biospin, Wissembourg (France)

O. Dakhlaoui
 Univ. Grenoble Alpes, CNRS, CERMAV
 38000 Grenoble (France)

Dr. J. van Tol, Dr. F. Mentink-Vigier
 National High Magnetic Field Laboratory, Florida State University,
 Tallahassee, FL 32301 (USA)
 E-mail: fmentink@magnet.fsu.edu

dubbed “AsymPol”.^[24] The efficiency of this family partly arises from the sizable dipolar and exchange interactions between the two electron spins. This property limits the depolarization effect,^[16] generates fast hyperpolarization build-ups and overall yields high MAS-DNP enhanced NMR sensitivities.^[24]

Despite advances in the design of new PAs, hyperpolarization of proton-dense systems is still a challenge. In other words, the impressive improvements of MAS-DNP, qualified on partially deuterated model systems, do not immediately translate in proton-dense systems such as organic powders and biomolecular systems. Here, we show that this problem is a consequence of the inappropriate assessment of the polarizing agents’ effectiveness and that it hinders the design of improved PAs. We illustrate this by comparing a new PA, cAsymPol-POK, to several known PAs while varying the number of protons to be polarized per biradical.

The new PA, cAsymPol-POK, in which the geminal methyl groups of the pyrrolinoxyl radical of AsymPol-POK^[24] are substituted with cyclohexyl groups, offers exceptional efficiency for proton-dense systems. Its performance is illustrated at high magnetic fields (9.4 to 18.8 T) and high MAS frequencies (10 to 40 kHz) for microcrystalline drugs and a 12.76 kDa protein. Its hyperpolarization ability enables high polarization levels for systems with short intrinsic bulk proton longitudinal relaxation times $T_{1,\text{H}}$ caused for example by the presence of methyl groups. The characteristics of cAsymPol-POK are demonstrated by MAS-DNP simulations, combined with electron paramagnetic resonance (EPR), density functional theory (DFT) and molecular dynamics (MD) calculations. They highlight the contribution of the two major conformers in AsymPol-POK and cAsymPol-POK, for which the variations of the electron-electron (e-e) dipolar coupling, the exchange interaction (J), as well as the relative orientation of the g -tensors are determined. A novel MAS-DNP simulation model also rationalizes their hyperpolarization capability for media that are difficult to hyperpolarize. Experiments performed with cAsymPol-POK have yielded timesaving up to a factor of 9, compared with AMUPol. This unlocks the acquisition, in only few hours, of short and long range 2D ^{13}C - ^{13}C and ^{15}N - ^{13}C correlation experiments at natural isotopic abundance (NA) of microcrystalline solids, here pharmaceutical drugs: the antibiotic ampicillin and the anti-inflammatory drug indomethacin. We also report excellent sensitivity on the 12.76 kDa U- ^{13}C , ^{15}N labeled sedimented LecA protein and present 2D spectra at 40 kHz MAS frequency recorded within minutes.

Results and Discussion

cAsymPol-POK: A New Member of the AsymPol Family

The “AsymPol family” has recently been introduced as an efficient family of PAs.^[24] The design of the chemical linker was guided by computational simulations and resulted in the generation of sizeable e–e couplings. For instance, AsymPol-

POK, the best water-soluble derivative reported in the previous study, is composed of a short tether with a conjugated carbon-carbon double bond in the 5-membered ring to improve the rigidity and provide a favorable relative orientation, by avoiding colinear nitroxide orientations. In addition, the two methyl groups of the piperidine-radical were replaced with spirocyclohexanoyl groups functionalized with phosphate moieties. To further tune the characteristics of AsymPol-POK, the geminal methyl groups of the pyrrolinoxyl radical were substituted by cyclohexyl groups in cAsymPol-POK. The removal of the methyl groups from the TEMPO moieties has already been investigated in the case of bCTbK,^[15] TEKPOL,^[16] AMUPol,^[14] bcTol,^[25] bcTol-M,^[25,26] cyolyl-TOTAPOL,^[14] and the TinyPol family.^[27]

The introduction of charged water-soluble moieties with AsymPol-POK (Figure 1) was crucial in its development and resulted not only in highly soluble PAs, but also prevented aggregation even at high concentration. In addition, increased molecular weight of biradicals can lengthen electron spin relaxation times,^[28–30] which is beneficial for CE MAS-DNP efficiency.^[31] In the case of cAsymPol-POK (Figure 1), first introduced here, the substitution of the geminal methyl groups in the pyrrolinoxyl radical by cyclohexyl-groups further improves the DNP efficiency of the AsymPol family.

Synthesis

The synthesis of cAsymPol-POK (Scheme 1) is similar to that of AsymPol-POK.^[24] First, TBDMS-protected spirocy-

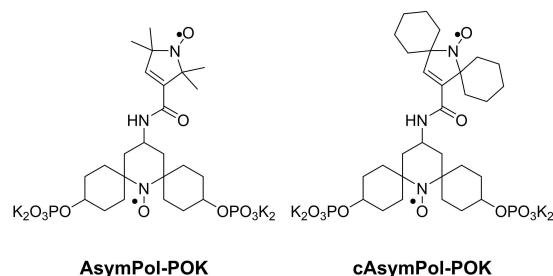
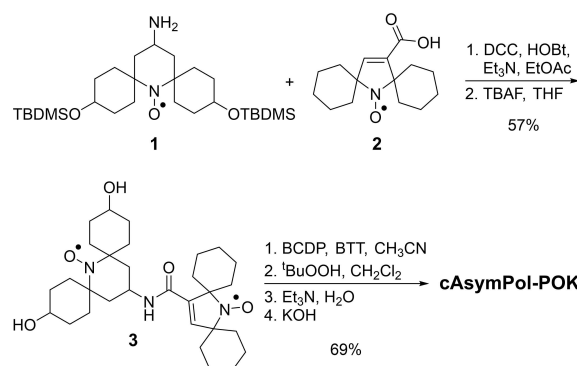


Figure 1. Chemical structure of AsymPol-POK and cAsymPol-POK.



Scheme 1. Synthesis of cAsymPol-POK. BCDP: bis(2-cyanoethyl)-*N,N*-diisopropyl-phosphoramidite, BTT: 5-benzylthio-1*H*-tetrazole.

clohexanoyl-amino-TEMPO **1** was conjugated to spirocyclohexyl-3-carboxypyrrolinoxyl nitroxide **2**, followed by removal of TBDMS protecting groups with TBAF to give compound **3**. Phosphitylation and deprotection of **3** gave cAsymPol-POK.

EPR and MAS-DNP Simulations for AsymPol-POK and cAsymPol-POK

In a previous study, we attempted to characterize the geometry and the magnetic properties of AsymPol-POK, but the resulting structure enabled only a partial match of the high field EPR spectrum and high values of exchange interaction were not accounted for.^[24] To better determine AsymPol-POK and cAsymPol-POK geometries, the EPR fit was carried out here starting from the predicted geometries given by DFT and MD calculations. DFT and MD calculations revealed that two conformers of both AsymPol-POK and cAsymPol-POK must be considered to fit the multi-frequency EPR data, yielding an excellent agreement between experiments and simulations, as shown in Figure 2b.

These conformers have similar relative energies and are thus approximately equally populated at low temperature. However, they lead to a different predicted exchange interaction and relative orientation of the nitroxides (see Supporting Information, Table S4). The DFT calculations also revealed that steric hindrance forces one of the spirocyclohexyls on the 5-membered ring to take a “closed conformation”.^[32] This fact was confirmed by X-ray crystallography (see Supporting Information, Figure S10). Conformer #1 has an exchange interaction $J_{a,b}$ of ≈ 120 MHz and ≈ 100 MHz for conformer #2. These values are significantly higher than in our previous assessment.^[24] Conformer #1 and #2 account for 55/45 % and 60/40 % for AsymPol-POK and cAsymPol-POK, respectively. Single-crystal X-ray analysis revealed only one conformer that is an “average” of conformer #1 and #2, and thus those conformers may only exist in glass forming matrices (see Supporting Information, Figure S10). Importantly, the numerical simulations predict that conformer #2 consistently performs better than conformer #1 but both conformers provide similar hyperpolarization build-up times (T_B). Thus, the introduction of the spirocyclohexyl rings on the pyrrolinoxyl radical in cAsymPol-POK has a negligible impact on the biradical geometry (i.e., cAsymPol-POK vs AsymPol-POK). The geometrical and magnetic parameters extracted from the EPR fit were also used to compute MAS-DNP field sweep profiles. As seen in Figure 2c, the simulations match well all the experimental data recorded at 9.4 T.

Assessing MAS-DNP Hyperpolarization Performance: The Returned Sensitivity

The MAS-DNP efficiency of a PA should not be solely judged by measuring the enhancement factor $\epsilon_{\text{On/Off}}$, i.e. the ratio between the NMR signal intensities with and without microwave irradiation.^[33] This ratio does not consider the

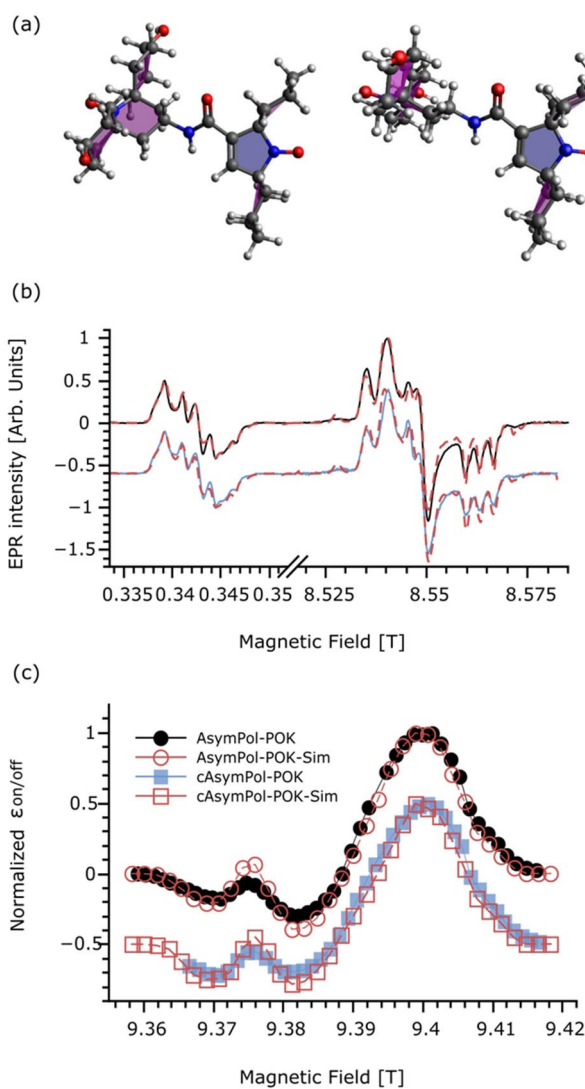


Figure 2. a) DFT-calculated structure of cAsymPol-OH viewed from the side, showing conformer #1 on the left and conformer #2 on the right. b) Concatenated X-band, 240 GHz EPR spectra and c) MAS-DNP field profile at 9.4 T for AsymPol-POK (black) and cAsymPol-POK (blue). The corresponding simulated EPR spectra and MAS-DNP field profiles are given as red dotted lines. For the MAS-DNP field profiles, experimental points are reported as circles for AsymPol-POK and squares for cAsymPol-POK, full for experiments and open for simulations.

time it takes to build-up the ^1H hyperpolarization (T_B) or depolarization (ϵ_{depo})/quenching factors that depend on the structure of the PA.^[16,33–35] Such correction factors should be evaluated to properly quantify the DNP gain compared to Boltzmann equilibrium, defined as $\epsilon_B = \epsilon_{\text{On/Off}} \epsilon_{\text{depo}}$.^[16] One can then define $\epsilon_B / \sqrt{T_B}$ as a measure of the relative sensitivity gain from DNP.^[33] However, the precise measurement of ϵ_{depo} , although very informative, is time-consuming and sensitive to the background signal of the probe.

Instead, it is more convenient to directly measure the returned sensitivity.^[4,36–40] It is defined as the hyperpolarized NMR signal intensity, detected in presence of microwave irradiation, per unit square root of time, for a given PA

concentration and sample amount. This quantification method provides a fair approach to compare the performance of different PAs and can be extended to applications where the polarization build-up curves are not mono-exponential.^[25,26]

Effect of the Proton Density on the DNP Enhancement Factor

$\epsilon_{\text{On/Off}}$

We tested the impact of the proton concentration by performing experiments in glass-forming matrices composed of glycerol and water. A high glycerol/water ratio (6:4 v/v) ensures a good and repeatable glass formation, necessary to conduct MAS-DNP experiments, and therefore kept constant. Two proton concentrations were tested, using either d_8 -glycerol/D₂O/H₂O (60:30:10 v/v, [¹H]=11 M), or glycerol/H₂O (60:40 v/v, [¹H]=110 M) as a DNP matrix. The first matrix is referred to as the, standard, *deuterated DNP matrix* and the second one as the *protonated DNP matrix*. Hyperpolarizing the protonated matrix is challenging since there are $\times 10$ more ¹H nuclei per biradical, and the ¹H $T_{1\rho}$ is also reduced from ≈ 70 s to 30 s.^[41,42] As shown in Table 1, the highest $\epsilon_{\text{On/Off}}$ value for AMUPol, measured at 8 kHz MAS and 14.1 T, is obtained in the standard deuterated matrix with $\epsilon_{\text{On/Off}} \approx 160$. Nevertheless, the depolarization factor is significant too, reaching approximately 0.5 at 14.1 T (see Supporting Information, Table S3), impacting the absolute polarization gain $\epsilon_B \approx 80$. This situation is very different for the radicals of the AsymPol family, that exhibit a small depolarization effect under the same experimental conditions of 0.78 and 0.77 for cAsymPol-POK and AsymPol-POK, respectively (see Supporting Information, Table S3). This limited depolarization, also predicted from the simulations (see Supporting Information, Table S5 and S6), is

Table 1: Experimental performance of 10 mM AMUPol, AsymPol-POK and cAsymPol-POK in the deuterated DNP matrix at 14.4 T, and 8 kHz MAS using a 3.2 mm rotor. The sensitivity was measured as $I_{\text{on}}(T_B)/\sqrt{T_B}$ with $I_{\text{on}}(T_B)$ the signal intensity measured for a same number of scans, the same sample amount, and an inter-scan delay set to $1.3T_B$. The sensitivity is normalized to the highest value.

	T_B [s]	$\epsilon_{\text{On/Off}}$	Sensitivity
AMUPol	4.8	160	0.7
AsymPol-POK	1.8	110	1
cAsymPol-POK	1.9	110	1

Table 2: Experimental performance of 10 mM AMUPol, AsymPol-POK and cAsymPol-POK in the protonated DNP matrix at 14.4 T, and 8 kHz MAS using a 3.2 mm rotor. The sensitivity was measured as $I_{\text{on}}(T_B)/\sqrt{T_B}$ with $I_{\text{on}}(T_B)$ the signal intensity measured for a same number of scans, the same sample amount, and an inter-scan delay set to $1.3T_B$. The sensitivity is normalized to the highest value.

	T_B [s]	$\epsilon_{\text{On/Off}}$	Sensitivity
AMUPol	6	120	0.4
AsymPol-POK	1.8	130	1
cAsymPol-POK	2	150	0.9

one of the important characteristics of the AsymPol family.^[24]

Interestingly, the values for the DNP enhancement factors $\epsilon_{\text{On/Off}}$ are very different when measuring the fully protonated matrix and even more so, they do not follow the same trend for AMUPol and the AsymPols at 8 kHz MAS and 14.1 T. The DNP enhancement factor of AMUPol is strongly reduced from ≈ 160 to ≈ 120 (Table 1 and 2), whereas it is increased for the AsymPol-POKs, from ≈ 110 to ≈ 130 for AsymPol-POK and from ≈ 110 to ≈ 150 for cAsymPol-POK. A decrease in $\epsilon_{\text{On/Off}}$, as observed for AMUPol, is expected as the ¹H bulk $T_{1\rho}$ (undoped) is shorter for the fully protonated matrix (cf. 70 vs 30 s). It is therefore surprising that the $\epsilon_{\text{On/Off}}$ values increase with the proton concentration of the matrix for both AsymPol-POK and cAsymPol-POK. A proper quantification of ϵ_B and ϵ_{depo} may explain these observations. However, in the fully protonated matrix, depolarization measurements are even more challenging due to radiation damping, and we were not able to quantify ϵ_{depo} . In the following, we therefore used the returned sensitivity instead.

Effect of the Proton Concentration on the DNP Build-Up Time

As shown in Table 1, the T_B is similar for both AsymPols (≈ 2 s) and much shorter than for AMUPol (4.8 s) at 10 mM PA concentration, at 14.1 T, and 8 kHz MAS. This feature is a direct consequence of the stronger e-e couplings (dipolar and exchange interaction) present in the AsymPols compared to AMUPol.^[24] Interestingly, the build-up time constants are unchanged for the AsymPols when going from 11 M to 110 M ¹H concentration (see Table 2). This is quite remarkable and proves the ability of these PAs to efficiently hyperpolarize a much larger number of protons. This is not the case for AMUPol, which requires a longer build-up time for 110 M proton concentration, as was also observed at 9.4 T.^[43] It is important to stress that a fast nuclear polarization build-up is essential to maximize the overall NMR sensitivity, and that the measured build-up time constants can be reproduced by MAS-DNP simulations (see Supporting Information, Table S5 and S6).

The Limits of Using a Deuterated Matrix for Benchmarking and Implications for the Design of Improved PAs

Beyond the MAS-DNP enhancement factor ($\epsilon_{\text{On/Off}}$), and build-up time constant (T_B), Table 1 and 2 also show the experimental DNP-enhanced NMR sensitivity at 14.1 T for both DNP matrices using the three radicals. Interestingly, the AsymPols yield a much higher sensitivity than AMUPol in both matrices, especially for the fully protonated one. This critical result highlights the importance of using sensitivity measurements to evaluate and compare radical efficiencies. It also underscores the importance of considering densely protonated matrices when the goal is to assess the efficiency of PAs for hyperpolarizing proton-rich samples. At 14.1 T and under moderate MAS frequency,

AsymPol-POK and cAsymPol-POK yield a similar sensitivity, which is $\times 1.4$ and $\times 2.5$ higher than AMUPol for a DNP matrix with proton concentration of 11 M and 110 M, respectively. This translates into an impressive $\times 6$ gain in timesaving for the fully protonated matrix. As shown below, the performance contrast between the AsymPols, in particular cAsymPol-POK, and AMUPol is even more striking at higher magnetic fields and faster spinning frequencies and/or when applied to organic microcrystals.

The Challenge of Polarizing Large, Protonated Microcrystals with DNP

The sensitivity offered by MAS-DNP has enabled numerous experiments that were previously unobtainable within reasonable time, such as structural studies of powdered organic samples at NA.^[8,44–46] 2D ^1H -X heteronuclear dipolar correlation spectra can be used to assign ^{13}C or ^{15}N resonances^[47] but they are not always resolved due to the low ^1H spectral resolution at the usually available MAS frequencies. ^{13}C - ^{13}C or ^{13}C - ^{15}N correlation experiments at NA offer better resolution but are very challenging, even when using MAS-DNP, due to the very low natural isotopic abundance of ^{13}C (1.1 %) and ^{15}N (0.4 %).^[8,36,44–46,48,49] Previous work has mostly been performed either on microcrystalline samples with sufficiently long bulk $T_{1,\text{n}}$,^[8,45,46] to allow large enhancements, or on nano-assemblies where one of the dimensions is in the nanometer scale, such as protein fibrils,^[44] cyclo-FF nanotubes,^[48] cellulose nanofibrils^[50] or whiskers,^[36] all of which are favorable for DNP experiments. However, the DNP efficiency decreases strongly with increasing particle size and/or in the presence of a short (few seconds) ^1H $T_{1,\text{n}}$ relaxation time (before doping), since the magnetization needs to diffuse from the surface of the particle to its core, while competing against returning to Boltzmann equilibrium.^[8] As such, organic microcrystals (micrometer size in all dimensions), in particular bearing methyl groups, are challenging targets and useful for testing new PAs.^[43,51]

cAsymPol-POK Can Efficiently Hyperpolarize Large Microcrystals with Short Nuclear Relaxation Time Constant $T_{1,\text{n}}$

AMUPol, AsymPol-POK and cAsymPol-POK were used to polarize microcrystals of the antibiotic ampicillin and the anti-inflammatory drug indomethacin, that possess a ^1H $T_{1,\text{n}}$ of 80 s and 3 s, respectively, at 9.4 T and 100 K. Both powders are sparingly soluble in water-based solvents and contain a relatively high proton concentration, ≈ 80 M for ampicillin and ≈ 58 M for indomethacin. SEM images of both powders confirm the presence of large micrometer-size crystals, especially in the case of indomethacin (see Supporting Information, Figure S5).

Several PA concentrations were tested, from 10 to 80 mM (Figure 3 and Supporting Information Figure S6) at 9.4 T. Interestingly, the sensitivity is optimal at around 40 mM radical solution for all three PAs. These results

correlate with those reported by Thureau et al.,^[52] where higher PA concentrations were used to suppress the solvent signals and improve the overall sensitivity. Figure 3 reports the returned sensitivity at the optimal recycle delay time T_{opt} (see Supporting Information, DNP build-up analysis) for the three radicals at 40 mM. It shows that the AsymPol PAs clearly outperform AMUPol in terms of sensitivity, with impressive short build-up times both at 9.4 T and at 14.1 T (Figure 3 and Supporting Information Figure S7).

In the case of ampicillin, the sensitivity is $\approx 90 \text{ s}^{-1/2}$ for cAsymPol-POK at 40 mM (see Figure 3a), which is about $\times 2.7$ higher than with AMUPol at 40 mM, corresponding to a factor of >7 in timesaving. Moreover, the corresponding optimal recycle delay time T_{opt} (Figure 3b) is much shorter for AsymPol-POK (2.8 s) and cAsymPol-POK (3.5 s), compared to 10.4 s for AMUPol (see Supporting Information, Tables S1 and S2 for the fitting of the build-up curves with a bi-exponential function, and calculation of T_{opt}). Similar conclusions can be drawn for indomethacin, which has a much shorter ^1H $T_{1,\text{n}}$. The sensitivity is, here too, optimal for cAsymPol-POK with a value of $\approx 36 \text{ s}^{-1/2}$, proving almost one order of magnitude in timesaving as compared to AMUPol. This result is remarkable, considering the much shorter ^1H $T_{1,\text{n}}$ of only 3 s for indomethacin.

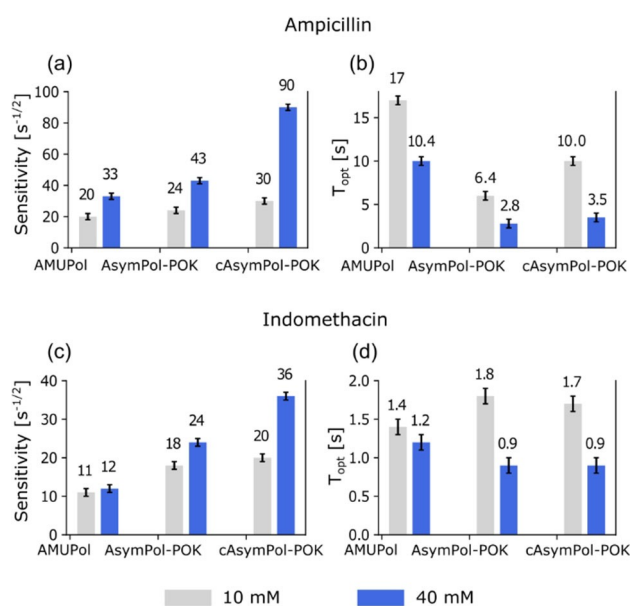


Figure 3. Experimental performance of a, b) ampicillin and c, d) indomethacin powders impregnated with 10 mM (grey) and 40 mM (blue) AMUPol, AsymPol-POK and cAsymPol-POK in the standard deuterated DNP matrix, d_3 -glycerol/ $\text{D}_2\text{O}/\text{H}_2\text{O}$ (60:30:10 v/v), at 105 K, 9.4 T and 8 kHz MAS. The plots show the signal-to-noise ratio per square root of the experimental time $(S/N)/\sqrt{t}$ in (a) and (c), and the optimal build-up time constant T_{opt} in (b) and (d) for ampicillin and indomethacin, respectively.

Unlocking NA ^{13}C - ^{13}C and ^{15}N - ^{13}C 2D Dipolar Correlation Spectroscopy of Microcrystals with cAsymPol-POK

The unprecedented sensitivity gain provided by 40 mM cAsymPol-POK enabled the acquisition of ^{13}C - ^{13}C double quantum-single quantum (DQ-SQ) and ^{15}N - ^{13}C dipolar correlation experiments for both ampicillin and indomethacin samples at NA in only a few hours (see Figure 4). It is worth noting that the signal-to-noise ratios of all 2D data

presented in Figure 4 are excellent, with corresponding experimental times in the range of 3 to 5 h.

The through-space ^{13}C - ^{13}C and ^{15}N - ^{13}C correlation spectra were recorded using the dipolar recoupling sequence SR26^[53] combined with StiC phase shifts^[48] and *z*f-TEDOR,^[54] respectively. Since dipolar truncation is statistically negligible in the case of NA samples, the mixing time was fixed to 4 ms to favor short through-space polarization transfer in both cases (equivalent to one or two bond lengths). Using the dataset in Figure 4, we were able to

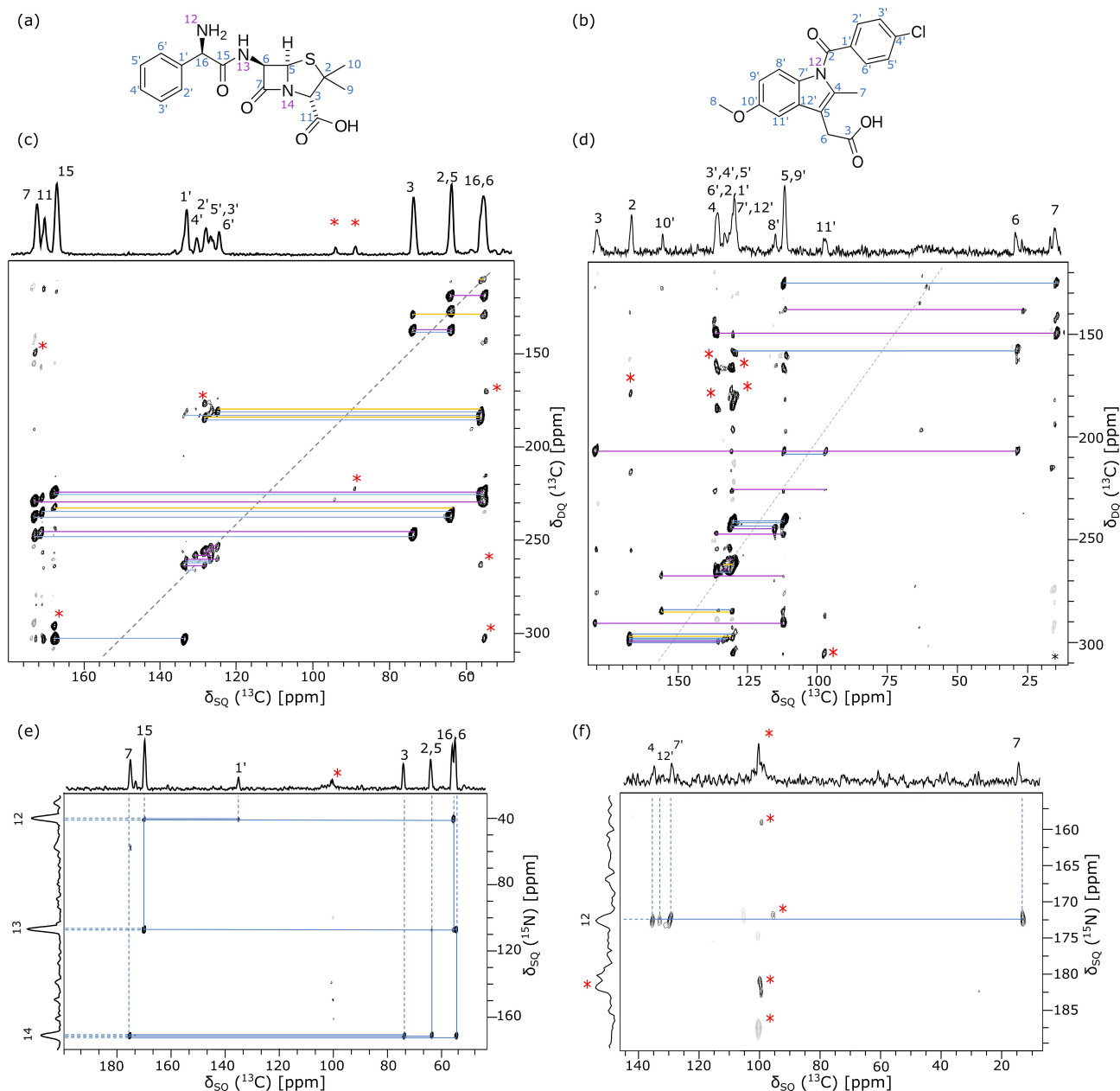


Figure 4. Molecular structures (a, b) and DNP-enhanced 2D ^{13}C - ^{13}C (c, d) and ^{15}N - ^{13}C (e, f) correlation spectra of ampicillin (a, c, e) and indomethacin (b, d, f) at NA. The DQ-SQ experiments in (c) and (d) were acquired using SR26 for dipolar recoupling, experiments in (e) and (f) were obtained with the *z*f-TEDOR sequence. All experiments were performed at 8 kHz MAS, 105 K and 9.4 T. Experimental times were 3 h for (b), 4 h for (c) and (d), and 5 h for (f). The ^{13}C assignment is mapped out in the 2D spectra, yielding one-bond (purple), two-bonds (blue) and three-bonds (yellow) correlations. Spinning side bands, signals from the carrier frequency and signals from the glycerol solvent are indicated with red asterisks.

Table 3: Experimental results of 10 mM cAsymPol-POK and AMUPol in a deuterated DNP matrix at magnetic field strengths of 9.4 and 18.8 T strength and high MAS frequency of 40 kHz. Note that the AMUPol reference sample was provided by the TGIR-RMN-THC FR3050 CNRS facility in Lyon.

	9.4 T, 1.3 mm rotor at 40 kHz			18.8 T, 1.3 mm rotor at 40 kHz		
	Norm. Sensitivity	T_B [s]	$\epsilon_{\text{On/Off}}$	Norm. Sensitivity	T_B [s]	$\epsilon_{\text{On/Off}}$
AMUPol	0.42	4.8	330	0.32	6	40
cAsymPol-POK	1	2.5	140	1	3.6	50

assign nearly all ^{13}C and ^{15}N resonances of both ampicillin and indomethacin. Correlations of the two methyl groups of ampicillin (carbon 9 and 10) and one of the methyl of indomethacin (carbon 8) could not be detected, which is often the case for measurements at 100 K.

AsymPol-POK and cAsymPol-POK Are Efficient PAs at High Magnetic Field and Fast MAS: Application to a Proton-Dense Biomolecular System

Additional experiments were conducted with a faster MAS frequency of 40 kHz at both 9.4 and 18.8 T (1.3 mm rotors). As expected, the AsymPol biradicals return large DNP

enhancements and relatively short build-up times. A quantitative comparison between AMUPol and cAsymPol-POK was conducted on a deuterated frozen solution at 40 kHz MAS (Table 3). It shows a $\times 2.4$ and $\times 3.1$ higher sensitivity compared to AMUPol, corresponding to a factor of ≈ 5.8 and ≈ 10 in timesaving at 9.4 and 18.8 T, respectively. This confirms the widening gap between cAsymPol-POK and AMUPol at increased magnetic fields, which is very promising for applications at fast and ultra-fast MAS.

This substantial improved sensitivity from cAsymPol-POK is accompanied with, once again, a short build-up time. This latter is $\approx 40\%$ shorter for cAsymPol-POK with respect to AMUPol at both 9.4 and 18.8 T, and 40 kHz MAS spinning. We note that high DNP enhancements were reported for the TinyPol family^[27] at 18.8 T and 40 kHz MAS on a deuterated matrix. However, these enhancements come at the cost of long build-up times of 13 s or more, compared to only 3.6 s in the case of cAsymPol-POK. The robustness of cAsymPol-POK at fast MAS and high magnetic fields can be directly attributed to the presence of a large exchange interaction between the electron spins, which is one of the main characteristics of the AsymPol family, confirmed by simulations at these regimes (See Supporting Information Table S4).

Finally, the performance of cAsymPol-POK at fast MAS was evaluated on a 12.76 kDa U- ^{13}C , ^{15}N labeled LecA protein. Such protein sample has a very dense proton content and a short $T_{1,n}$ of ≈ 7 s, mainly due to the presence of numerous methyl groups. At 40 kHz MAS and using 32 mM cAsymPol-POK, a large enhancement factor of $\epsilon_{\text{On/Off}} = 130$ with an impressively short T_B of 0.5 s were obtained on the LecA sample (Figure 5a). Interestingly, the returned enhancement factor is similar to the one obtained for a deuterated frozen solution (Table 3), highlighting the effectiveness of cAsymPol-POK to polarize targets that are proton-rich and have relatively short ^1H $T_{1,n}$. Figure 5b shows a 2D ^{13}C - ^{13}C SQ-SQ DARR^[55] spectrum with an excellent signal-to-noise ratio, acquired at 40 kHz MAS with less than 1 mg of protein in 19 min of experimental time. Such impressive DNP signal enhancements are particularly important for emerging biomolecular applications, in particular if they can be combined with Targeted DNP and Selective DNP approaches.^[7,56]

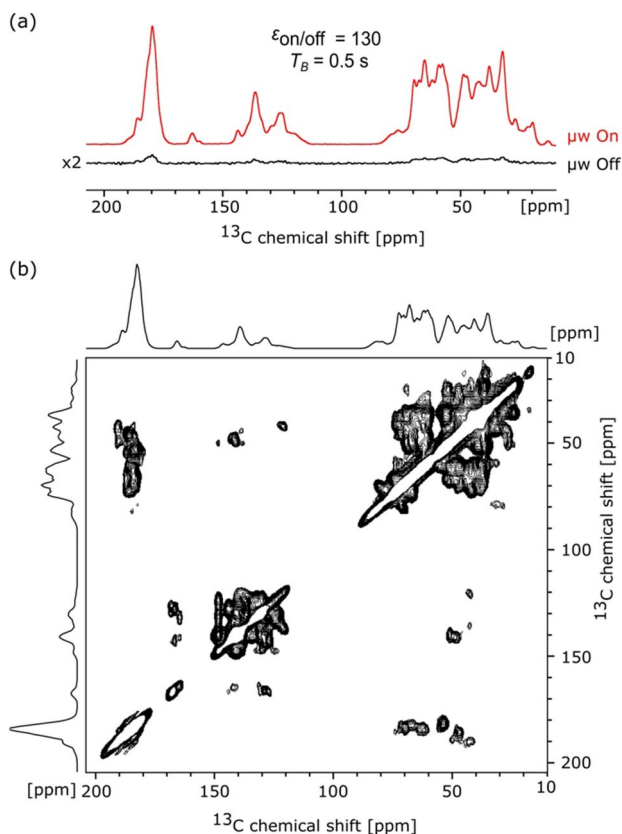


Figure 5. a) ^1H - ^{13}C CP-MAS spectra with (red) and without (black) μw irradiation of U- ^{13}C , ^{15}N LecA, leading to an enhancement factor $\epsilon_{\text{On/Off}}$ of 130. b) DNP-enhanced 2D SQ-SQ ^{13}C - ^{13}C correlation spectrum using the DARR sequence of the U- ^{13}C , ^{15}N LecA. All spectra were acquired at a MAS frequency of 40 kHz, 9.4 T and 106 K.

Conclusion

In this work, we provide a rationale for the limited DNP efficiency of PAs developed thus far for NMR studies of proton-dense molecular solids. Part of the problem originates from the fact that common PAs have been benchmarked and selected based on their performance for solutes in matrices with low proton density. Such deuterated matrices also have a long ^1H $T_{1\rho}$ and are thus relatively easy to hyperpolarize, while also being prone to amplifying depolarization effects present with some PAs. This triggered the report of large DNP enhancement factors, which do not always correlate with large DNP NMR sensitivity. Keeping this in mind, we introduced here a new polarizing agent, cAsymPol-POK, which provides outstanding efficiency for proton-dense molecular systems at high magnetic fields (up to 18.8 T) and fast MAS frequencies (up to 40 kHz). This new biradical is compatible with challenging biomolecular applications and unlocks the rapid acquisition of ^{13}C – ^{13}C and ^{15}N – ^{13}C correlation experiments on pharmaceutical drugs at natural isotopic abundance, which are key experiments for structure determination. The performance of cAsymPol-POK is rationalized by MAS-DNP simulations, combined with EPR, DFT and MD calculations. They show that the introduction of the spirocyclohexyl groups does not significantly change the linker geometry, nor the e–e spin couplings involved. Thus, the improved performance of cAsymPol-POK relative to AsymPol-POK is attributed to the replacement of methyl groups with cyclohexyl groups, which tends to lengthen both the electron and the core protons relaxation times leading to better CE-DNP efficiency.^[14–16,25–27]

Acknowledgements

This work was supported by the French National Research Agency (CBH-EUR-GS and Labex ARCANÉ ANR-17-EURE-0003, Glyco@Alps ANR-15-IDEX-02, and ANR-16-CE11-0030-03) and the European Research Council Grant ERC-CoG-2015 No. 682895 to G.D.P. Part of this work, carried out on the Platform for Nanocharacterisation (PFNC), was supported by the “Recherches Technologiques de Base” program of the French National Research Agency (ANR). This work was supported by the Icelandic Research Fund, grant No. 173727, and the University of Iceland Research Fund (S.Th.S). T.H. thanks the Deutsche Forschungsgemeinschaft (DFG) for a postdoctoral fellowship (414196920). The National High Magnetic Field Laboratory is supported by the NSF (DMR-1157490 and DMR-1644779) and by the State of Florida. The 14.1 T DNP system at NHMFL is funded in part by NIH S10 OD018519 (magnet and console), NSF CHE-1229170 (gyrotron), and NIH P41GM122698. FMV thanks Shimon Vega for all the discussion related to the Cross-effect mechanism. Financial support from the TGIR-RMN-THC Fr3050 CNRS for conducting DNP experiments at high magnetic fields (18.8 T) is gratefully acknowledged.

Conflict of Interest

The authors declare no conflict of interest

Keywords: Biomolecules • Dynamic Nuclear Polarization • MAS-DNP • Nuclear Magnetic Resonance • Pharmaceuticals • Polarizing Agents

- [1] D. D. Laws, H.-M. L. Bitter, A. Jerschow, *Angew. Chem. Int. Ed.* **2002**, *41*, 3096–3129.
- [2] B. Reif, S. E. Ashbrook, L. Emsley, M. Hong, *Nat. Rev. Methods Primer* **2021**, *1*, 1–23.
- [3] A. S. Lilly Thankamony, J. J. Wittmann, M. Kaushik, B. Corzilius, *Prog. Nucl. Magn. Reson. Spectrosc.* **2017**, *102*, 120–195.
- [4] D. Lee, S. Hediger, G. De Paëpe, *Solid State Nucl. Magn. Reson.* **2015**, *66*, 6–20.
- [5] Q. Z. Ni, E. Daviso, T. V. Can, E. Markhasin, S. K. Jawla, T. M. Swager, R. J. Temkin, J. Herzfeld, R. G. Griffin, *Acc. Chem. Res.* **2013**, *46*, 1933–1941.
- [6] B. Plainchont, P. Berruyer, J.-N. Dumez, S. Jannin, P. Giraudeau, *Anal. Chem.* **2018**, *90*, 3639–3650.
- [7] D. Gauto, O. Dakhlaoui, I. Marin-Montesinos, S. Hediger, G. D. Paëpe, *Chem. Sci.* **2021**, *12*, 6223–6237.
- [8] A. J. Rossini, A. Zagdoun, F. Hegner, M. Schwarzwälder, D. Gajan, C. Copéret, A. Lesage, L. Emsley, *J. Am. Chem. Soc.* **2012**, *134*, 16899–16908.
- [9] K. Jaudzems, T. Polenova, G. Pintacuda, H. Oschkinat, A. Lesage, *J. Struct. Biol.* **2019**, *206*, 90–98.
- [10] K. N. Hu, H. H. Yu, T. M. Swager, R. G. Griffin, *J. Am. Chem. Soc.* **2004**, *126*, 10844–10845.
- [11] H. Karoui, O. Ouari, G. Casano, *Emagres* **2018**, *7*, 195–207.
- [12] A. B. Barnes, G. De Paëpe, P. C. A. Van Der Wel, K. N. Hu, C. G. Joo, V. S. Bajaj, M. L. Mak-Jurkauskas, J. R. Sirigiri, J. Herzfeld, R. J. Temkin, R. G. Griffin, *Appl. Magn. Reson.* **2008**, *34*, 237–263.
- [13] C. Song, K. N. Hu, C. G. Joo, T. M. Swager, R. G. Griffin, *J. Am. Chem. Soc.* **2006**, *128*, 11385–11390.
- [14] C. Sauvée, M. Rosay, G. Casano, F. Aussenac, R. T. Weber, O. Ouari, P. Tordo, *Angew. Chem. Int. Ed.* **2013**, *52*, 10858–10861; *Angew. Chem.* **2013**, *125*, 11058–11061.
- [15] A. Zagdoun, G. Casano, O. Ouari, M. Schwarzwälder, A. J. Rossini, F. Aussenac, M. Yulikov, G. Jeschke, C. Copéret, A. Lesage, P. Tordo, L. Emsley, *J. Am. Chem. Soc.* **2013**, *135*, 12790–12797.
- [16] F. Mentink-Vigier, S. Paul, D. Lee, A. Feintuch, S. Hediger, S. Vega, G. De Paëpe, *Phys. Chem. Chem. Phys.* **2015**, *17*, 21824–21836.
- [17] S. R. Chaudhari, P. Berruyer, D. Gajan, C. Reiter, F. Engelke, D. L. Silverio, C. Copéret, M. Lelli, A. Lesage, L. Emsley, *Phys. Chem. Chem. Phys.* **2016**, *18*, 10616–10622.
- [18] D. Mance, P. Gast, M. Huber, M. Baldus, K. L. Ivanov, *J. Chem. Phys.* **2015**, *142*, 234201.
- [19] G. Mathies, M. A. Caporini, V. K. Michaelis, Y. Liu, K. N. Hu, D. Mance, J. L. Zweier, M. Rosay, M. Baldus, R. G. Griffin, *Angew. Chem. Int. Ed.* **2015**, *54*, 11770–11774; *Angew. Chem.* **2015**, *127*, 11936–11940.
- [20] F. Mentink-Vigier, G. Mathies, Y. Liu, A. L. Barra, M. A. Caporini, D. Lee, S. Hediger, R. Griffin, G. De Paëpe, *Chem. Sci.* **2017**, *8*, 8150–8163.
- [21] W. Zhai, A. Lucini Paioni, X. Cai, S. Narasimhan, J. Medeiros-Silva, W. Zhang, A. Rockenbauer, M. Weingarth, Y. Song, M. Baldus, Y. Liu, *J. Phys. Chem. B* **2020**, *124*, 9047–9060.
- [22] D. Wissler, G. Karthikeyan, A. Lund, G. Casano, H. Karoui, M. Yulikov, G. Menzildjian, A. C. Pinon, A. A. Purea, F. Engelke,

- S. R. Chaudhari, D. Kubicki, A. J. Rossini, I. B. Moroz, D. Gajan, C. Copéret, G. Jeschke, M. Lelli, L. Emsley, A. Lesage, O. Ouari, *J. Am. Chem. Soc.* **2018**, *140*, 13340–13349.
- [23] P. Berruyer, S. Björgvinsdóttir, A. Bertarello, G. Stevanato, Y. Rao, G. Karthikeyan, G. Casano, O. Ouari, M. Lelli, C. Reiter, F. Engelke, L. Emsley, *J. Phys. Chem. Lett.* **2020**, *11*, 8386–8391.
- [24] F. Mentink-Vigier, I. Marin-Montesinos, A. P. Jagtap, T. Halbritter, J. Van Tol, S. Hediger, D. Lee, S. T. Sigurdsson, G. De Paëpe, *J. Am. Chem. Soc.* **2018**, *140*, 11013–11019.
- [25] A. P. Jagtap, M. A. Geiger, D. Stöppler, M. Orwick-Rydmark, H. Oschkinat, S. T. Sigurdsson, *Chem. Commun.* **2016**, *52*, 7020–7023.
- [26] M. A. Geiger, A. P. Jagtap, M. Kaushik, H. Sun, D. Stöppler, S. T. Sigurdsson, B. Corzilius, H. Oschkinat, *Chem. Eur. J.* **2018**, *24*, 13485–13494.
- [27] A. Lund, G. Casano, G. Menzildjian, M. Kaushik, G. Stevanato, M. Yulikov, R. Jabbour, D. Wisser, M. Renom-Carrasco, C. Thieuleux, F. Bernada, H. Karoui, D. Siri, M. Rosay, I. V. Sergeev, D. Gajan, M. Lelli, L. Emsley, O. Ouari, A. Lesage, *Chem. Sci.* **2020**, *11*, 2810–2818.
- [28] H. Sato, V. Kathirvelu, A. Fielding, J. P. Blinco, A. S. Micallef, S. E. Bottle, S. S. Eaton, G. R. Eaton, *Mol. Phys.* **2007**, *105*, 2137–2151.
- [29] A. Zagdoun, G. Casano, O. Ouari, G. Lapadula, A. J. Rossini, M. Lelli, M. Baffert, D. Gajan, L. Veyre, W. E. Maas, M. Rosay, R. T. Weber, C. Thieuleux, C. Copéret, A. Lesage, P. Tordo, L. Emsley, *J. Am. Chem. Soc.* **2012**, *134*, 2284–2291.
- [30] V. Kathirvelu, C. Smith, C. Parks, M. A. Mannan, Y. Miura, K. Takeshita, S. S. Eaton, G. R. Eaton, *Chem. Commun.* **2009**, 454–456.
- [31] K. R. Thurber, R. Tycko, *J. Chem. Phys.* **2012**, *137*, 084508.
- [32] G. Stevanato, G. Casano, D. J. Kubicki, Y. Rao, L. E. Hofer, G. Menzildjian, H. Karoui, D. Siri, M. Cordova, M. Yulikov, G. Jeschke, M. Lelli, A. Lesage, O. Ouari, L. Emsley, *J. Am. Chem. Soc.* **2020**, *142*, 16587–16599.
- [33] S. Hediger, D. Lee, F. Mentink-Vigier, G. De Paëpe, *eMagRes* **2018**, *7*, 105–116.
- [34] K. R. Thurber, R. Tycko, *J. Chem. Phys.* **2014**, *140*, 184201.
- [35] B. Corzilius, L. B. Andreas, A. A. Smith, Q. Z. Ni, R. G. Griffin, *J. Magn. Reson.* **2014**, *240*, 113–123.
- [36] H. Takahashi, D. Lee, L. Dubois, M. Bardet, S. Hediger, G. De Paëpe, *Angew. Chem. Int. Ed.* **2012**, *51*, 11766–11769; *Angew. Chem.* **2012**, *124*, 11936–11939.
- [37] M.-A. Geiger, M. Orwick-Rydmark, K. Märker, W. T. Franks, D. Akhmetzyanov, D. Stöppler, M. Zinke, E. Specker, M. Nazaré, A. Diehl, B.-J. van Rossum, F. Aussenac, T. Prisner, Ü. Akbey, H. Oschkinat, *Phys. Chem. Chem. Phys.* **2016**, *18*, 30696–30704.
- [38] A. J. Rossini, A. Zagdoun, M. Lelli, D. Gajan, F. Rascón, M. Rosay, W. E. Maas, C. Copéret, A. Lesage, L. Emsley, *Chem Sci* **2012**, *3*, 108–115.
- [39] T. Kobayashi, O. Lafon, A. S. Lilly Thankamony, I. I. Slowing, K. Kandel, D. Carnevale, V. Vitzthum, H. Vezin, J.-P. Amoureux, G. Bodenhausen, M. Pruski, *Phys. Chem. Chem. Phys.* **2013**, *15*, 5553.
- [40] F. A. Perras, L.-L. Wang, J. S. Manzano, U. Chaudhary, N. N. Opembe, D. D. Johnson, I. I. Slowing, M. Pruski, *Curr. Opin. Colloid Interface Sci.* **2018**, *33*, 9–18.
- [41] F. Mentink-Vigier, U. Akbey, Y. Hovav, S. Vega, H. Oschkinat, A. Feintuch, *J. Magn. Reson.* **1997** **2012**, *224*, 13–21.
- [42] F. Mentink-Vigier, S. Vega, G. D. Paëpe, *Phys. Chem. Chem. Phys.* **2017**, *19*, 3506–3522.
- [43] N. A. Prisco, A. C. Pinon, L. Emsley, B. F. Chmelka, *Phys. Chem. Chem. Phys.* **2021**, *23*, 1006–1020.
- [44] A. N. Smith, K. Märker, S. Hediger, G. De Paëpe, *J. Phys. Chem. Lett.* **2019**, *10*, 4652–4662.
- [45] K. Märker, M. Pingret, J. M. Mouesca, D. Gasparutto, S. Hediger, G. De Paëpe, *J. Am. Chem. Soc.* **2015**, *137*, 13796–13799.
- [46] A. J. Rossini, C. M. Widdifield, A. Zagdoun, M. Lelli, M. Schwarzwälder, C. Copéret, A. Lesage, L. Emsley, *J. Am. Chem. Soc.* **2014**, *136*, 2324–2334.
- [47] A. Lesage, P. Charmont, S. Steuernagel, L. Emsley, *J. Am. Chem. Soc.* **2000**, *122*, 9739–9744.
- [48] K. Märker, S. Hediger, G. De Paëpe, *Chem. Commun.* **2017**, 53, 9155–9158.
- [49] H. Takahashi, C. Fernández-De-Alba, D. Lee, V. Maurel, S. Gambarelli, M. Bardet, S. Hediger, A. L. Barra, G. De Paëpe, *J. Magn. Reson.* **2014**, *239*, 91–99.
- [50] A. Kumar, H. Durand, E. Zeno, C. Balsollier, B. Watbled, C. Sillard, S. Fort, I. Baussanne, N. Belgacem, D. Lee, S. Hediger, M. Demeunynck, J. Bras, G. De Paëpe, *Chem. Sci.* **2020**, *11*, 3868–3877.
- [51] Y. Matsuki, T. Kobayashi, J. Fukazawa, F. A. Perras, M. Pruski, T. Fujiwara, *Phys. Chem. Chem. Phys.* **2021**, *23*, 4919–4926.
- [52] P. Thureau, M. Juramy, F. Ziarelli, S. Viel, G. Mollica, *Solid State Nucl. Magn. Reson.* **2019**, *99*, 15–19.
- [53] P. E. Kristiansen, M. Carravetta, J. D. Van Beek, W. C. Lai, M. H. Levitt, *J. Chem. Phys.* **2006**, *124*, 234510.
- [54] C. P. Jaronec, C. Filip, R. G. Griffin, *J. Am. Chem. Soc.* **2002**, *124*, 10728–10742.
- [55] K. Takegoshi, S. Nakamura, T. Terao, *Chem. Phys. Lett.* **2001**, *344*, 631–637.
- [56] I. Marin-Montesinos, D. Goyard, E. Gillon, O. Renaudet, A. Imberty, S. Hediger, G. De Paëpe, *Chem. Sci.* **2019**, *10*, 3366–3374.

Manuscript received: October 18, 2021

Accepted manuscript online: January 12, 2022

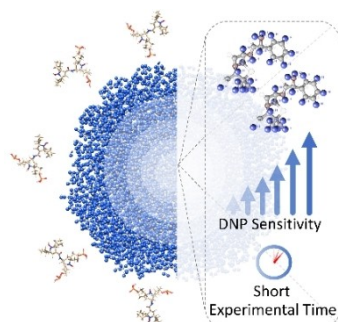
Version of record online: ■■■, ■■■

Research Articles

Solid-State NMR

R. Harrabi, T. Halbritter, F. Aussenac,
O. Dakhlaoui, J. van Tol, K. K. Damodaran,
D. Lee, S. Paul, S. Hediger, F. Mentink-
Vigier,* S. T. Sigurdsson,*
G. De Paëpe* ————— e202114103

Highly Efficient Polarizing Agents for MAS-
DNP of Proton-Dense Molecular Solids



A new polarizing agent is introduced to efficiently polarize proton-dense solids through dynamic nuclear polarization (DNP) ssNMR. This work shows that this new biradical can be used on organic microcrystals and biomolecular assemblies at high field and fast magic angle spinning (MAS). It notably unlocks the rapid acquisition of ^{13}C - ^{13}C and ^{15}N - ^{13}C correlations of pharmaceutical drugs at natural isotopic abundance, which are key experiments for structure determination.